Can the Nonadiabatic Photodynamics of Aminopyrimidine Be a Model for the Ultrafast Deactivation of Adenine?

Mario Barbatti* and Hans Lischka*

Institute for Theoretical Chemistry, University of Vienna, Waehringerstrasse 17, A-1090, Vienna, Austria

Received: January 5, 2007; In Final Form: February 12, 2007

The reaction path for the ultrafast deactivation of 6-aminopyrimidine (6AP) has been investigated by means of ab initio surface-hopping dynamics. The electronic vertical excitation spectrum, excited-state S_1 minima, and minima on the crossing seam of 6AP resemble well those found for adenine. The deactivation from the S_1 to the S_0 state takes place at the ultrafast time scale of 400 fs and involves the out-of-plane ring deformation of the C_4 atom, a position that is sterically restricted in adenine by the imidazole ring. Mechanical restrictions have been used to simulate in a simple way the role of the imidazole group in adenine. As a result, deactivation via out-of-plane ring deformation of the C_2 and N_3 atoms are observed in good agreement with predictions for adenine. These dynamics results show that the previously suggested ring puckering deactivation paths really exist at a time scale, which is compatible with experimentally observed life times. The electronic structure of the crossing seam has been shown to have the same nature as those of simple biradicaloid systems, a feature which seems to be valid for any cyclic system.

1. Introduction

The photodynamical behavior of DNA and RNA bases is of great interest and has been studied intensively in recent years.[1−5] After UV photoexcitation the DNA and RNA bases return to the electronic ground state at an ultrafast time scale of about 1 ps.[5] Their short excited-state lifetimes imply an intrinsic stability against structural photoinduced changes. Since the bases decay quickly to the electronic ground state, they do not have time enough to undergo structural deformation induced by the reactive excited states. The excess of electronic energy will be converted into vibrational energy and transferred to the environment. This fast deactivation mechanism is expected to play a significant role not only for the photostability of the bases themselves but also for that of the DNA and RNA, reducing the risk of structural damage and mutations.[6]

In particular, for adenine, theoretical investigations have shown that at least three types of deactivation paths exist connecting the excited state to the ground state through conical intersections. The first type of path is given by the out-of-plane ring deformation, which leads to a crossing region between the $^1\pi\pi^*$ and the closed-shell ($^1\pi^2$) ground states.[7−11] The second type of deactivation path involves strong out-of-plane motions of the amino group resulting in a crossing assigned as $^1n\pi^*/^1\pi^2$.[7,8] Finally, the third type of deactivation path is given by the NH, OH, or ring-CN stretchings, which have been shown by Sobolewski and Domcke[12] and Perun, Sobolewski, and Domcke[13] to lead to a crossing between the $^1\pi\sigma^*$ state and the ground state. For energetic reasons, one has argued that the most probable deactivation path dominating in low excitation energies is the puckering of the C_2H group (see Chart 1).[8,9,13] The central role of the C_2 site can also be deduced from the very long lifetime of 2-aminopurine,[5] indicating that the new position of the amino group inhibits the deformation at the C_2 site.

CHART 1

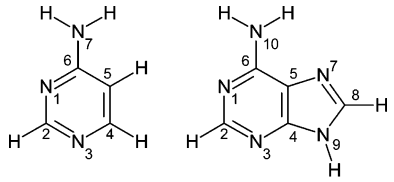

In the last years, there have been several experimental and theoretical attempts to understand the properties of the Watson−Crick pairs based on smaller model systems such as 7-azaindole dimmer,[14,15] 2-aminopyridine dimmer,[16] and the pair 2-pyridone-2-aminopyridine.[17,18] Since the pyrimidine ring plays a central role in the chemical structure of all five DNA and RNA bases, we wanted to investigate the possibilities for constructing suitable base models based on this heterocycle. From a computational point of view, smaller models have the advantage of reduced computing times, an issue that is of special importance for the dynamics calculations performed in this work. In particular concerning the photochemistry of adenine, 6-aminopyrimidine (6AP) looks as a natural candidate for such a model system (see Chart 1). Besides the role of 6AP as a reduced adenine model, the study of its photochemical properties is an interesting topic of its own because of the importance of the pyrimidine heterocycle in organic chemistry.[19−21]

Most of the theoretical investigations on the photostability of DNA bases have used static approaches describing the most important points on the energy surface (energy minima, minima on the crossing seam (MXS)) or selected reaction paths. Even though these calculations have been of fundamental importance for the current understanding of the deactivation processes, they alone cannot give full information about time-dependent properties, such as lifetimes and specific reaction paths actually realized in the course of the deactivation process. In the present work we are taking one major step toward the photodynamical simulation of DNA bases by performing surface-hopping

* To whom correspondence should be addressed. E-mail: mario.barbatti@univie.ac.at (M.B.); hans.lischka@univie.ac.at (H.L.).

10.1021/jp070089w CCC: $37.00
Published on Web 03/24/2007

TABLE 1: Excitation Energies of 6AP Computed at the Optimized Geometries of the Ground State, of Three Different Minima of the S_1 State, and of the Minima on the Crossing Seam (Geometries Were Optimized at SA-3-CAS(8,7)/6-31G* Level and Results for 9H-Ade are Also Shown)

		6AP ΔE (eV)			
state	geometry[a]	CAS(8,7)[b]	CAS(10,8)[c]	MR-QDPT2[d]	9H-Ade ΔE (eV)
$S_0\,\pi^2$	min. S_0	0.00	0.00	0.00	0.00
$S_1\,\pi\pi^*$	min. S_0	5.34	5.34	4.79	5.23[e], 4.85[f], 4.90[g]
S_2 nπ^*	min. S_0	5.88	5.43	4.71	6.19[e], 5.50[f], 5.01[g]
S_1	min. $S_1\,\pi\pi$*	5.06	5.07	4.51	5.18[e], 4.48[f]
S_1	min. S_1 nπ* C_2	5.02	4.88	4.33	5.15[e], 4.69[f]
S_1	min. S_1 nπ* C_4	4.93	4.82	4.22	
S_0/S_1	MXS C_2	4.49	4.52	4.36	~4.3[e], ~3.8[f], 4.64[h]
S_0/S_1	MXS C_4	4.79	4.79	4.71	
S_0/S_1	MXS C_6	4.60	4.60	4.62	~4.6[e], ~4.1[f], 4.81[h]

[a] Cartesian geometries of all stationary points and the MXSs of 6AP are available in the Supporting Information. [b] SA-3-CAS(8,7)/6-31G*. $E_0 = -317.803765$ au. [c] SA-3-CAS(10,8)/6-31G*. $E_0 = -317.805043$ au. [d] MR-QDPT2/SA-3-CAS(10,8)/6-31G*. $E_0 = -318.724360$ au. [e] CAS(12,10) calculations, ref 7. [f] CASPT2 calculations, ref 7. [g] DFT/MRCI calculations, ref 9. [h] SA-2-CAS(12,10)/6-31G* present calculations using the geometries of ref 8.

calculations on 6AP as a model system. These calculations aim at realistic simulations of 6AP under particular consideration of the following two aspects. One of them is the fact that a direct or on-the-fly approach[22,23] is used, which allows straightforward inclusion of all internal degrees of freedom into the dynamics calculation without any preselection depending on external model assumptions. The second aspect is the fact that the electronic structure calculations are based, within manageable limits, on flexible quantum chemical approaches (complete active space self-consistent field (SA-CASSCF) and a polarized basis set). In addition to these dynamics calculations, the nature of the electronic structure in the crossing seam region has been explored in order to understand the general role of the ring deformation for the deactivation of heteroaromatic rings.

2. Computational Details and Methods

On-the-fly (or direct) ab initio nonadiabatic dynamics calculations have been performed for 6AP using Tully's surface hopping approach.[24] A total of 80 trajectories were simulated. The nuclear motion was obtained within the classical approximation by solving Newton's equations using the Born−Oppenheimer potential. The integration of the classical equations was done by means of the Velocity−Verlet algorithm[25] in time steps of 0.5 fs. For the integration of the time-dependent Schrödinger equation (TDSE) for the electrons,[26] each time step was further divided into 15 sub-time-steps and integrated by means of the fifth-order Butcher algorithm.[27] The adiabatic representation was used to expand the time-dependent wave function including two singlet electronic states, S_0 and S_1. The time-dependent population of each electronic state was employed to obtain the probability of electronic transition according to the improved fewest switches algorithm proposed by Hammes-Schiffer and Tully.[28] At each sub-time-step, a random event was used to decide whether the system will switch to another state. The initial conditions for the trajectories simulated were generated by means of a ground-state quantum harmonic oscillator distribution of nuclear coordinates. The nuclear momentum was scaled so as to reproduce the zero-point energy in the harmonic approximation.

Energy gradients required for the integration of Newton's equations as well as the nonadiabatic coupling vectors necessary for the integration of the TDSE were obtained by analytic procedures described in refs 29−31 using the state-averaged (SA) CASSCF method. Eight electrons and seven orbitals were included in the active space [CAS(8,7)]. This space is composed of one lone pair orbital n and six π orbitals. In the ground-state equilibrium geometry, the n orbital is mostly centered at the N_3 site, but during the dynamics, the active space showed to be flexible enough to automatically localize this orbital on the N_1 site when necessary. Three singlet states (SA-3) were included in the state averaging procedure. The effect of the inclusion of the second n orbital in the active space was investigated for selected points at the SA-3-CAS(10,8) level. Additional single-point calculations were performed for 9H-adenine (9H-Ade) at the SA-2-CAS(12,10) level and for $CH_2NH_2^+$ at the SA-3-CAS(4,3) level. The multireference quasidegenerate second-order perturbation theory (MR-QDPT2)[32] was used to check the effect of dynamical electron correlation in 6AP. The 6-31G* basis set[33] was used in all calculations.

The dynamics simulations were performed with the NEWTON-X package.[23,34] The COLUMBUS program system[35−37] was used for the CASSCF calculations. The AO integrals were computed using DALTON.[38] MR-QDPT2 calculations were performed with the GAMESS package.[39]

3. Results and Discussion

3.1. Potential Energy Surfaces (PESs). Vertical excitation energies, stationary points on the energy surface of the first excited-state, and the conical intersections (minima on the crossing seam) have been computed for 6AP.

In Table 1 the CASSCF results computed with 8 electrons and 7 orbitals [CAS(8,7)], which is the level used in the dynamics calculations, are compared with the results obtained with 10 electrons and 8 orbitals [CAS(10,8)]. Both sets of results agree quite well. At the vertical excitation, they show the S_1 state with $\pi\pi$* character, closely followed by the S_2 state with nπ* character. Three minima on the S_1 surface are characterized in Table 1 The S_1 minimum with $\pi\pi$* character has almost planar geometry, while the two minima with nπ* character shows some degree of puckering at the C_2 and C_4 sites. As expected, the inclusion of an additional n orbital into the CAS(8,7) to form the CAS(10,8) has the general effect of stabilizing the ^{1}nπ* state. Nevertheless, the data show that there is no qualitative change when comparing the results of the two sets of calculations. This is a good indication that the CAS(8,7) level can be adequately used in the dynamics calculations.

It has been shown for adenine that inclusion of dynamical electron correlation through the CASPT2 method only displaces all CASSCF S_1 excitation energies uniformly by approximately 0.5 eV.[7] This conclusion can also be reached from the detailed comparison between CASSCF and CASPT2 results for 9H-Ade that has been conducted by Chen and Li (see Supporting

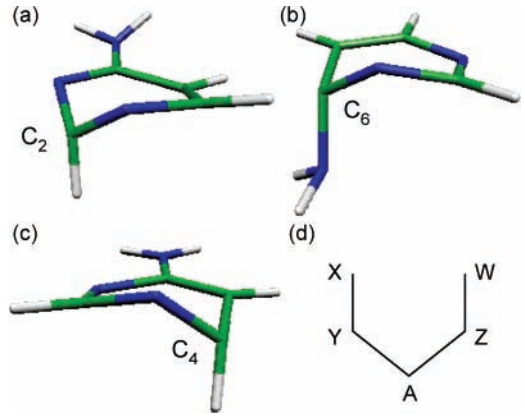

Figure 1. MXS based on out-of-plane deformations at the sites (a) C_2, (b) C_6, and (c) C_4. (d) Scheme of bonds near the deformed site.

Information of ref 8). Their results for several cuts along the PES show that dynamical correlation has a drastic effect on the second $^1\pi\pi^*$ state, which is strongly stabilized, resulting in an entanglement of the S_2 and S_3 states. Nevertheless, the energies of the S_1 and S_0 states are only vertically displaced and the shapes of the potential energy curves are barely affected. The situation is similar for 6AP, as we can see from the comparison of the CASSCF and MR-QDPT2 energies in Table 1. In these two methods the S_1 state is stabilized by practically the same amount of energy when going from the vertical excitation to the energy minimum. The MXS energies, however, are stabilized to a smaller amount by the MR-QDPT2 method. This implies that the lifetime of the systems should be longer if dynamical electron correlation were included. This analysis shows that the inclusion of dynamical correlation, although desirable, is not mandatory in the current simulations, since 6AP is initially excited in the S_1 state and remains in S_1 up to crossing to the ground state.

Different ordering of the $\pi\pi^*$ and $n\pi^*$ states between the CASSCF and the MR-QDPT2 calculations is found (see Table 1). The wide distribution in vertical excitations obtained for adenine as shown in Table 1 demonstrate the difficulties with the calculation of vertical energies in this case. We should note, however, that whatever the character of the S_1 state is, the exit of the Franck−Condon region will be descending toward the $n\pi^*$ minimum. The trajectories will relax to this region before they find the path to the intersection. In the course of this relaxation, which may take hundreds of femtoseconds (see section 3.2), it is expected that the memory concerning differences in the character of the initial S_1 state in the Franck−Condon region is largely lost. Nevertheless, it is planned to address this issue in more detail in the future.

Out-of-plane deformations (puckering) at C_2, C_4, and C_6 sites of 6AP produce a crossing between the ground and S_1 states. The geometries of the minimum on the crossing seam (MXS) for each case are displayed in Figure 1 and its energies are given in Table 1. Additional information on these MXSs is given in Table 2, which is discussed in detail in Section 3.4.

It is not surprising to find that the topography of the first excited-state of 6AP and 9H-Ade are quite similar. On the S_1 surface, the planar relaxation of 9H-Ade leads to a $^1\pi\pi^*$ minimum[7,8] similar to that in 6AP (Table 1). Furthermore, similar to 6AP, out-of-plane deformation of 9H-Ade at the C_2 site leads also to an additional minimum on the S_1 surface, which has $n\pi^*$ character. It has been shown[7−9] that puckering of adenine in the C_2 and C_6 sites also produces conical intersections. Even the reaction path connecting the vertical excitation region to the MXS shows strong similarities, as can be seen from Figure 3, which will be discussed later. One non-negligible difference, however, comes from the puckering at the C_4 site, which produces a S_0/S_1 crossing for 6AP while it is not feasible for 9H-Ade at reasonable energies due to the restriction imposed by the imidazole group. We shall see in section 3.2 that this difference is important for using 6AP as a model for 9H-Ade.

TABLE 2: Characterization of MXS Structures in 6AP and Adenine

MXS	twisted bonds	dihedral angle (deg)
C_2	C_2N_3	$(N_1C_2N_3C_4) = 73$
	C_2N_1	$(N_3C_2N_1C_6) = 61$
C_4	C_4N_3	$(C_2N_3C_4C_5) = 67$
	C_4C_5	$(N_3C_4C_5C_6) = 45$
C_6	C_6N_1	$(C_2N_1C_6C_5) = 63$
	C_6C_5	$(N_1C_6C_5C_4) = 43$
		$(C_2N_1C_6N) = 67$
Ade C_2[a]	C_2N_3	$(N_1C_2N_3C_4) = 70$
	C_2N_1	$(C_6N_1C_2N_3) = 68$
Ade C_6[a]	C_6N_1	$(C_2N_1C_6C_5) = 58$
	C_6C_5	$(N_1C_6C_5C_4) = 33$
		$(C_2N_1C_6N) = 69$

[a] Reference 8.

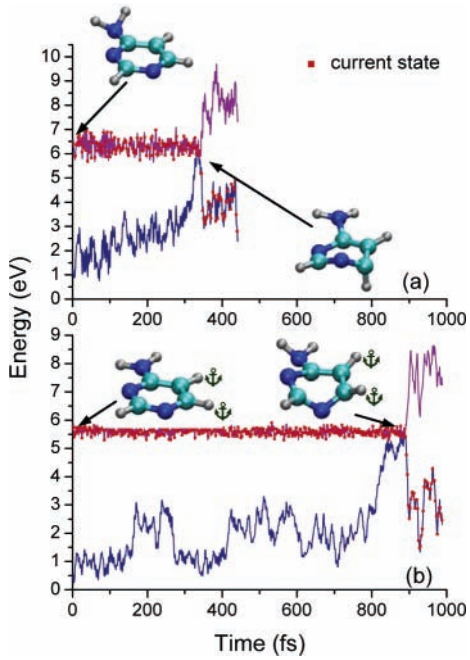

Figure 2. S_0 and S_1 energies of two typical surface-hopping trajectories for (a) 6AP and (b) isotopically substituted 6AP. Dots indicate the current state in each time. The anchors indicate the substituted atoms.

3.2. Nonadiabatic Dynamics of 6AP. Surface-hopping dynamics calculations have been performed for a total of 80 trajectories and a maximum simulation period of 800 fs. Each individual trajectory was stopped as soon as 6AP jumped to the ground state and remained in it for more than 100 fs. Our primary goal was the characterization of the actual low-energy main deactivation path and not the computation of highly accurate life times. To accomplish that, 30 trajectories were run for normal 6AP without any isotopic substitution. After starting the trajectories in the S_1 ($^1\pi\pi^*$) state, 6AP quickly returned to the ground state. The average lifetime was 416 ± 150 fs. The 5 trajectories (17%) that did not return to the ground state at all after 800 fs were excluded from this average. The reaction path driving 6AP to the S_0/S_1 intersection mainly involves the puckering at the C_4H group. The respective MXS structure is shown in Figure 1c (see also Table 2).

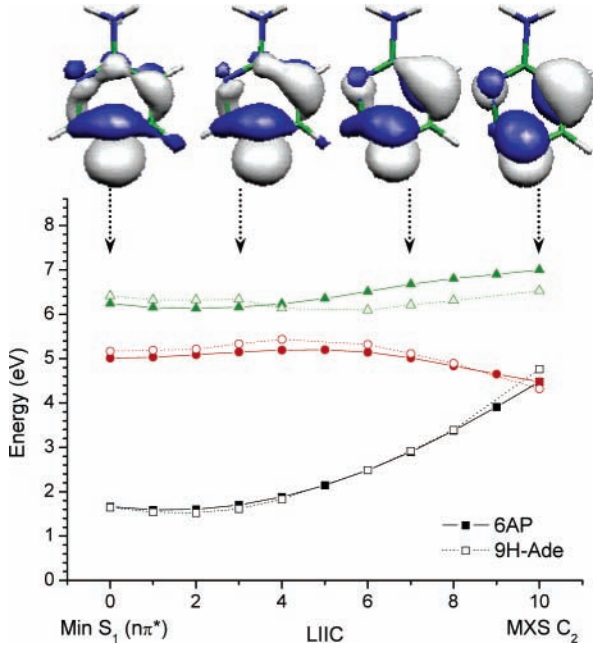

Figure 3. Reaction path between the minimum on S_1 ($n\pi^*$ C_2) and the MXS C_2 of 6AP, obtained by LIIC. The dashed lines show the equivalent results for 9H-Ade of ref 7. The change in character of the singly occupied molecular orbital A (see text) is shown for selected points of the path.

In the first stage of the dynamics (the first 100 fs), 6AP maintains planarity and the character of the S_1 state frequently oscillates between $\pi\pi^*$ and $n\pi^*$. After that, the character of the S_1 state stabilizes as $n\pi^*$. The puckering starts at around 300 fs, when the character of the state changes again to $\pi\pi^*$ and the system quickly reaches a region of crossing between the $^1\pi\pi^*$ state and the ground state, into which the system decays. This process is exemplified in Figure 2a. Although about 75% of the trajectories that decay have followed this path, another 25% follow the out-of-plane deformation involving the C_2H and N_3 sites. None of the trajectories followed the NH_2-out-of-plane or the NH-stretching paths.

The changes in the character of the S_1 state can be better understood in terms of a reaction path. In Figure 3 the path obtained by linear interpolation of internal coordinates (LIIC) between the S_1 ($n\pi^*$ C_2) minimum and the MXS C_2 for 6AP is plotted. Although in the dynamics the puckering occurs mostly at the C_4 site, the path to MXS C_2 is plotted for the purpose of direct comparison with the equivalent path for 9H-Ade, as given in ref 7. The same conclusions, however, apply for both C_2 and C_4 puckerings, as will be discussed in section 3.4. At point 0 of the path, the S_1 state is predominantly of $n\pi^*$ character. Along the path, the mixing between the n character and the π character gradually increases until the π character starts to be the dominant one, and the state ends up as $\pi\pi^*$ in the region of crossing. Thus, in the biradicaloid S_1 state, characterized by the singly occupied orbitals A and B, the orbital A (plotted in Figure 3) transforms from n into π along the path, while the orbital B keeps its π^* nature.

The fact that the S_0/S_1 crossing occurs at the C_4 site, corresponding to the MXS of highest energy (Table 1) is remarkable. Nevertheless, as we have discussed elsewhere[40] for ethylene (see also ref 41), the system often hops in regions of the crossing seam that are energetically far from the MXS. Therefore, the detailed energies of the MXSs are not so important for the determination of the actual crossing in comparison to other features of the reaction paths driving the system in the excited state.

3.3. Effect of Mechanical Restrictions on the Dynamics. The predominance of the nonadiabatic deactivation involving the C_4H group discussed in the previous section is not favorable for using 6AP as a model for adenine. In adenine, the imidazole group is connected to the C_4 and C_5 sites to form the purine group, and we cannot expect any strong out-of-plane deformation there due to structural restrictions. One possible way of dealing theoretically with this problem, but still keeping the simplicity of the 6AP model, is to increase the isotopic masses of the H atoms attached to the C_4 and C_5 sites, simulating in this way the increased rigidity at these points. We used "heavy" hydrogen atoms to simulate the mechanical restrictions of the imidazole group, in a procedure analogous to that one used by Warshel in the simulation of restricted retinal.[42] The isotopic mass of the hydrogen atoms at the C_4 and C_5 sites was chosen to be 45 amu. This value produces a moment of inertia for the out-of-plane motion that equals the moment of inertia of the center-of-mass of the imidazole group.

A new set of 30 trajectories including the isotopic substitutions has been computed for a simulation period of 1700 fs. The initial conditions for these trajectories were resampled using the frequencies and the normal modes of the substituted species. As before, each individual trajectory was stopped as soon as the system jumped to the ground state and remained in it for more than 100 fs. The isotopic substitution has a significant effect on the dynamics simulations. The lifetime averaged over the 23 trajectories that hop to the ground state increases to 957 $\pm$ 200 fs, which is a value notably similar to the experimental lifetime of adenine (1.0 ps[5]). The potential energies of a typical trajectory are shown in Figure 2b. The puckering at the C_4H group was almost completely inhibited, and the main path to the crossing seam is the out-of-plane deformation involving the C_2 and N_3 sites. Now the most commonly accessed conical intersections resemble the MXSs shown in Figure 1a. Seven trajectories (23%) did not arrive at any crossing within 1.7 ps and did not return to the ground state. Again, none of the trajectories followed the NH_2-out-of-plane or the NH-stretching paths.

The lack of activation of the NH_2-out-of-plane path can be explained in terms of (1) the big moment of inertia of this group, which inhibits the strong out-of-plane deformations necessary to reach the crossing seam and (2) the energy barrier along the reaction path.[7,8,13] We have tried to check whether one of these reasons is the dominant one by performing dynamics simulations using a smaller mass for the N atom of the NH_2 group and, therefore, a smaller moment of inertia in the amino group. This change does not affect the PES, which is independent of the nuclear masses. Nevertheless, this change will have an effect on the kinetic energy and the regions of the energy surface visited. We set the mass of nitrogen to 1 amu and performed two series of 10 trajectories, the first one without any change in the masses of the H atoms attached to the C_4 and C_5 sites, and the second one with mechanical restrictions at these sites as well. Also in these calculations, we did not observe any activation of the NH_2 out-of-plane path in any of the 20 trajectories, and the hoppings to the ground state occurred in the ways described above. The average of the absolute value of the NH_2 out-of-plane angle (angle between N_7 and the $C_6N_1C_5$ plane) in the normal 6AP is 2° with the maximum value reaching 7°. After the reduction of the N mass, the average increases to 3.5° and the maximum value to 13°. The mechanical restriction at C_4 and C_5 sites did not affect these values. All these angles

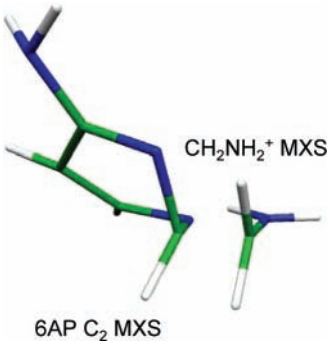

Figure 4. MXS of 6AP (left) and $CH_2NH_2^+$ (right).

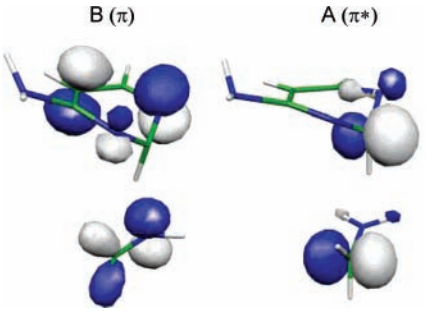

Figure 5. π and the π* orbitals of 6AP and $CH_2NH_2^+$ at their respective MXS geometries.

are by far too small in comparison to the out-of-plane angle at the crossing seam region, which assumes a value of 44° in the C_6 MXS shown in Figure 1b. Our conclusion is that, since the NH_2 moment of inertia plays a minor role in the inhibition of this path, the barriers arising from the electronic structure interactions between the amino group and the pyrimidine group are essential for the inhibition of the path, which is in line with the conclusions of ref 13 for adenine.

3.4. Electronic Structure of the Crossing Seam. All paths conducting 6AP to the crossing seam involve strong out-of-plane deformations. Similar conical intersections have also been predicted for uracil,[43] 9H-Ade,[7−9] 2-aminopurine,[44] cytosine,[45] pyrazine,[46] thymine,[47] and benzene.[46,48−50] Perun, Sobolewski, and Domcke[7] have suggested that these intersections, which appear always at the same kind of out-of-plane deformation, could be a general property of six-membered aromatic and heteroaromatic rings. Recently, we have shown that this kind of intersection also occurs in 5-membered rings.[51]

Interestingly enough, the origin of such crossings seems to depend more on the biradicaloid character of the S_1 state than on the cyclic features of the molecules. Indeed, these crossings have the same nature as the crossings in simple polar π bonds. Michl and Bonačić-Koutecký[52] have shown that by twisting a biradicaloid such as $\pi\pi$*-excited $CH_2NH_2^+$ (Figure 4 right) by 90°, a crossing between the S_1 and S_0 states is produced. On the basis of a simple two-electron two-orbital model, they have determined the conditions that need to be satisfied by two perturbative parameters to achieve the crossing. In polar systems with localized and approximately non-interacting active orbitals such as $CH_2NH_2^+$,[52,53] CH_2CHF,[54] or CH_2SiH_2,[55] these conditions are approximately satisfied by a simple rigid torsion. In nonpolar systems such as ethylene, the sudden polarization triggered by the pyramidalization[56] or hydrogen migration coordinates[57] can be used to tune the conditions to obtain the S_1/S_0 crossing.[58]

The same analysis seems to be applicable to ring systems. Inspection of the conical intersections of 9H-Ade and 6AP shows that their out-of-plane deformations approximately twist the C═N or C═C bonds as in the biradicaloid ethylenic systems. This fact has been pointed out also by Zgierski et al.[20] in their analysis of cytosine and uracil. Let us take, for example, the S_0/S_1 crossing at C_2H puckering (Figure 1a). A different view of this MXS is plotted in Figure 4 for easier comparison with the biradicaloid methaniminium cation ($CH_2NH_2^+$). In Figure 5 the singly occupied orbitals are plotted in comparison with those of $CH_2NH_2^+$. In the C_2 MXS, the C_2N_3 and the C_2N_1 bonds are twisted in such a way that the $N_1C_2N_3C_4$ and the $N_3C_2N_1C_6$ dihedral angles are 73 and 61°, respectively (Table 2). At this point, the wave functions of the two degenerate states are characterized by the closed shell $|B^2>$ and the biradical $|A^1B^1>$ configurations, where A is a p-like orbital centered on C_2 (Figure 5, right) and B is a p-like orbital centered on N_1 with additional contributions centered on N_3 and C_5 (Figure 5, left). Note that, since the plane of the ring was destroyed by the puckering, it is not possible to uniquely assign B as a lone pair or as a π orbital. The same is true for the orbital A. However, the torsional angles in combination with the analysis of the electronic wave functions of the two intersecting states strongly suggest the analogy with the torsion of a π system and not with isolated lone pairs. The biradicaloid character of the system can be confirmed also by the natural occupancies of the open-shell orbitals, which are approximately 0.8 and 1.5 (state averaged).

Exactly the same analysis, including the dominant configurations, the orbital shapes and occupancies, the assignments, and the dihedral angle values, is valid for all other crossings found in 6AP, including the C_6 MXS. In this latter case, the out-of-plane position of the amino group alone has nothing directly to do with the crossing itself, but both, crossing and position of the amino group, are consequences of the bond twisting in the ring.

The fact that the S_0/S_1 crossing is a consequence of the twisting of the bonds rather than of a puckering around some specific site implies that the crossing can be reached in a large variety of geometrical configurations, quite different from those shown in Figure 1. As has been often observed during the dynamics, the twisting of bonds can result, for instance, in conical intersections that have two or more centers moved out of the ring plane.

We want to draw attention to some subtle differences between the NC and CC twisting in the ring. For NC bonds, the nuclear conformation should be close to the 90°-twisted geometry to tune the crossing. For CC bonds, however, the atomic configuration should be pyramidalized in order to produce the same effect. As a result, the dihedral angles around the NC bonds are much bigger than the dihedral angles around the CC bonds, as can be seen in Table 2.

Normally, the crossing seam shows a complex topography. Similar to conventional geometry optimization, the search for conical intersections depends strongly on the initial guess, which will determine which local minimum on the crossing seam will be found. From the discussion in this section, we can envisage a general procedure to generate initial guesses to locate several puckered MXSs of cyclic systems. Starting from the ground-state equilibrium geometry:

1. Take one of the vertices of the ring (A, in Figure 1d) and displace it out of the plane. If YA (or AZ) is a CC bond, the final XYAZ (or YAZW) dihedral angle should be approximately 45°. If YA (or AZ) is a NC bond, the final XYAZ (or YAZW) dihedral angle should be approximately 65°.

2. Use the geometry obtained at step 1 as the initial guess in the MXS search.

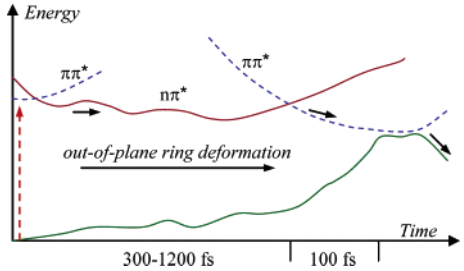

Figure 6. Schematic view of the photodynamics of 6AP in the S_1 state. In the first part of the dynamics, 300 fs refers to normal 6AP, while 1200 fs refers to the isotopically substituted species (see text).

3. Repeat steps 1 and 2 to each vertex belonging to only one ring.

Obviously, this procedure is not useful in the localization of S_1/S_0 intersections arising from NH and NC stretchings, although it has been useful to find open-ring conical intersections in 5-memebered rings.[51]

4. Conclusions

We have studied the ultrafast nonadiabatic deactivation of 6AP by means of on-the-fly surface-hopping dynamics at the CASSCF level. The dynamics of 6AP can be summarized in the following way (see Figure 6): during the motion on the S_1 surface, the system moves to a region of nπ* character. 6AP stays trapped in this nπ* region for a few hundred femtosenconds until the out-of-plane deformation at C_4 changes the character of the S_1 state to $\pi\pi$*. As soon as this happens, the system moves quickly toward the crossing seam, across which it returns to the ground state. The corresponding lifetime is about 400 fs.

Deactivation through the just-mentioned out-of-plane deformation at C_4 means that, in spite of its similarities with 9H-Ade, 6AP cannot be directly used as a model for the photodynamics of 9H-Ade, since in the latter case the puckering at the C_4 site cannot happen due to restrictions imposed by the imidazole ring. In an attempt to emulate the presence of the imidazole ring, simulations with artificial isotopic substitution in 6AP have been performed. The masses of the hydrogen atoms at C_4 and C_5 were adjusted in order to provide them with the same moment of inertia as in adenine. In this case 6AP expends much more time in the nπ* region until out-of-plane deformation in the sites N_3 and C_2 takes place, regions which are also expected to be relevant for the ultrafast de-excitation of adenine. A lifetime of about 1 ps is obtained in this case, a value that is notably similar to the experimental lifetime of adenine.

Thus, at least partially 6AP can be used as a quite useful model for adenine. It can be concluded that the previously suggested ring puckering deactivation paths are really available also for 9H-Ade at a time scale, which is compatible with experimentally observed life times. It is clear, however, that for accurate simulations of the photodynamics of adenine, our approximate procedure is not sufficient and that the entire purine structure of adenine has to be taken into account.

The motion toward the crossing seam is composed of the twisting of two adjacent bonds, which moves one or two atomic sites strongly out of the plane of the aromatic ring. After finding the path to perform the twisting, the system spends no longer than 100 fs until it approaches the crossing with the ground state, mainly by destabilization of the ground state. The electronic structure of the crossing seam can be understood in terms of the biradicaloid character of the S_1 surface and the crossing itself is produced by conjugate torsional motion of some polar bonds. This is a general result that seems to be valid in principle for any cyclic system and provides a general method to search for conical intersections.

Acknowledgment. The authors thank Prof. C. Marian for helpful discussions. This work was supported by the Austrian Science Fund within the framework of the Special Research Program F16 (Advanced Light Sources) and Project P18411-N19. We are grateful for technical support and computer time at the Linux PC cluster Schrödinger III of the computer center of the University of Vienna.

Supporting Information Available: Potential energy curves, molecular orbitals, Cartesian coordinates of stationary points and MXSs, CASSCF energies, initial conditions for trajectories of Figure 2. This material is available free of charge via the Internet at http://pubs.acs.org.

References and Notes

(1) Kang, H.; Lee, K. T.; Jung, B.; Ko, Y. J.; Kim, S. K. *J. Am. Chem. Soc.* **2002**, *124*, 12958.
(2) Kang, H.; Jung, B.; Kim, S. K. *J. Chem. Phys.* **2003**, *118*, 6717.
(3) Ullrich, S.; Schultz, T.; Zgierski, M. Z.; Stolow, A. *J. Am. Chem. Soc.* **2004**, *126*, 2262.
(4) Crespo-Hernandez, C. E.; Cohen, B.; Hare, P. M.; Kohler, B. *Chem. Rev.* **2004**, *104*, 1977.
(5) Canuel, C.; Mons, M.; Piuzzi, F.; Tardivel, B.; Dimicoli, I.; Elhanine, M. *J. Chem. Phys.* **2005**, *122*, 074316.
(6) Broo, A. *J. Phys. Chem. A* **1998**, *102*, 526.
(7) Perun, S.; Sobolewski, A. L.; Domcke, W. *J. A. Chem. Soc.* **2005**, *127*, 6257.
(8) Chen, H.; Li. S. *J. Phys. Chem. A* **2005**, *109*, 8443.
(9) Marian, C. *J. Chem. Phys.* **2005**, *122*, 104314.
(10) Nielsen, S. B.; Sølling, T. I. *Chem. Phys. Chem.* **2005**, *6*, 1276.
(11) Serrano-Andrés, L.; Merchán, M.; Borin, A. C. *Proc. Natl. Acad. Sci., U.S.A.* **2006**, *103*, 8691.
(12) Sobolewski, A. L.; Domcke, W. *Eur. J. Phys. D* **2002**, *20*, 369.
(13) Perun, S.; Sobolewski, A. L.; Domcke, W. *Chem. Phys.* **2005**, *313*, 107.
(14) Douhal, A.; Kim, S. K.: Zewail, A. H. *Nature* **1995**, *378*, 260.
(15) Fiebig, T.; Chachisvilis, M.; Manger, M.; Zewail, A. H.; Douhal, A.; Garcia-Ochoa, I.; de La Hoz Ayuso, A. *J. Phys. Chem. A* **1999**, *103*, 7419.
(16) Schultz, T.; Samoylova, E.; Radloff, W.; Hertel, I. V.; Sobolewski, A. L.; Domcke, W. *Science* **2004**, *306*, 1765.
(17) Müller, A.; Talbot, F.; Leutwyler, S. *J. Am. Chem. Soc.* **2002**, *124*, 14486.
(18) Frey, J. A.; Müller, A.; Frey, H.-M.; Leutwyler, S. *J. Chem. Phys.* **2004**, *121*, 8237.
(19) Lagoja, I. M. *Chem. Biodiv.* **2005**, *2*, 1.
(20) Zgierski, M. Z.; Patchkovskii, S.; Fujiwara, T.; Lim, E. C. *J. Phys. Chem. A* **2005**, *109*, 9384.
(21) Lin, M.-F.; Dyakov, Y. A.; Tseng, C.-M.; Mebel, A. M.; Lin, S. H.; Lee, Y. T.; Ni, C.-K. *J. Chem. Phys.* **2006**, *124*, 084303.
(22) (a) Vreven, T.; Bernardi, F.; Garavelli, M.; Olivucci, M.; Robb, M. A.; Schlegel, H. B. *J. Am. Chem. Soc.* **1997**, *119*, 12687. (b) Ciminelli, C.; Granucci, G.; Persico, M. *Chem.−Eur. J.* **2004**, *10*, 2327. (c) Jasper, A. W.; Truhlar, D. G. *J. Chem. Phys.* **2005**, *122*, 044101. (d) Mitrić, R.; Bonačić-Koutecký, V.; Pittner, J.; Lischka, H. *J. Chem. Phys.* **2006**, *125*, 024303.
(23) Barbatti, M.; Granucci, G.; Persico, M.; Ruckenbauer, M.; Vazdar, M.; Eckert-Maksiae, M.; Lischka, H. *J. Photochem. Photobiol. A* **2007**, in press, doi:10.1016/j.jphotochem.2006.12.008.
(24) Tully, J. C. *J. Chem. Phys.* **1990**, *93*, 1061.
(25) Swope, W. C.; Andersen, H. C.; Berens, P. H.; Wilson, K. R. *J. Chem. Phys.* **1982**, *76*, 637.
(26) Ferretti, A.; Granucci, G.; Lami, A.; Persico, M.; Villani, G. *J. Chem. Phys.* **1996**, *104*, 5517.
(27) Butcher, J. *J. Assoc. Comput. Mach.* **1965**, *12*, 124.
(28) Hammes-Schiffer, S.; Tully, J. C. *J. Chem. Phys.* **1994**, *101*, 4657.
(29) Shepard, R. In *Modern Electronic Structure Theory Part I*; Yarkony, D. R., Ed.; World Scientific: Singapore, 1995; p 345.
(30) (a) Shepard, R.; Lischka, H.; Szalay, P. G.; Kovar, T.; Ernzerhof, M. *J. Chem. Phys.* **1992**, *96*, 2085. (b) Lischka, H.; Dallos, M.; Shepard, R. *Mol. Phys.* **2002**, *100*, 1647.

(31) (a) Lischka, H.; Dallos, M.; Szalay, P. G.; Yarkony, D. R.; Shepard, R. *J. Chem. Phys.* **2004**, *120*, 7322. (b) Dallos, M.; Lischka, H.; Shepard, R.; Yarkony, D. R.; Szalay, P. G. *J. Chem. Phys.* **2004**, *120*, 7330.

(32) Nakano, H. *J. Chem. Phys.* **1993**, *99*, 7983.

(33) (a) Hehre, W. J.; Ditchfield, R.; Pople, J. A. *J. Chem. Phys.* **1972**, *56*, 2257. (b) Hariharan, P. C. Pople, J. A. *Theor. Chim. Acta.* **1973**, *28*, 213.

(34) Barbatti, M.; Granucci, G.; Lischka, H.; Ruckenbauer, M.; Persico, M. *NEWTON-X: a package for Newtonian dynamics close to the crossing seam, version 0.11b*, **2006,** www.univie.ac.at/newtonx.

(35) Lischka, H.; Shepard, R.; Brown, F. B.; Shavitt, I. *Int. J. Quantum Chem.* **1981**, *15*, 91.

(36) Lischka, H.; Shepard, R.; Shavitt, I.; Pitzer, R. M.; Dallos, M.; Mueller, Th.; Szalay, P. G.; Brown, F. B.; Ahlrichs, R.; Boehm, H. J.; Chang, A.; Comeau, D. C.; Gdanitz, R.; Dachsel, H.; Ehrhardt, C.; Ernzerhof, M.; Hoechtl, P.; Irle, S.; Kedziora, G.; Kovar, T.; Parasuk, V.; Pepper, M. J. M.; Scharf, P.; Schiffer, H.; Schindler, M.; Schueler, M.; Seth, M.; Stahlberg, E. A.; Zhao, J.-G.; Yabushita, S.; Zhang, Z.; Barbatti, M.; Matsika, S.; Schuurmann, M.; Yarkony, D. R.; Brozell, S. R.; Beck, E. V.; Blaudeau, J.-P. *COLUMBUS, an ab initio electronic structure program, release 5.9.1*, 2006. www.univie.ac.at/columbus

(37) (a) Shepard, R.; Shavitt, I.; Pitzer, R. M.; Comeau, D. C.; Pepper, M.; Lischka, H.; Szalay, P. G.; Ahlrichs, R.; Brown, F. B.; Zhao, J. *Int. J. Quantum Chem.* **1988**, *22*, 149. (b) Lischka, H.; Shepard, R.; Pitzer, R. M.; Shavitt, I.; Dallos, M.; Müller, Th.; Szalay, P. G.; Seth, M.; Kedziora, G. S.; Yabushita, S.; Zhang, Z. *Phys. Chem. Chem. Phys.* **2001**, *3*, 664.

(38) Helgaker, T.; Jensen, H. J. Aa.; Jørgensen, P.; Olsen, J.; Ruud, K.; Ågren, H.; Andersen, T.; Bak, K. L.; Bakken, V.; Christiansen, O.; Dahle, P.; Dalskov, E. K.; Enevoldsen, T.; Heiberg, H.; Hettema, H.; Jonsson, D.; Kirpekar, S.; Kobayashi, R.; Koch, H.; Mikkelsen, K. V.; Norman, P.; Packer, M. J.; Saue, T.; Taylor, P. R.; Vahtras, O. *DALTON, an ab initio electronic structure program, Release 1.0*, **1997**.

(39) Schmidt, M. W.; Baldridge, K. K.; Boatz, J. A.; Elbert, S. T.; Gordon, M. S.; Jensen, J. J.; Koseki, S.; Matsunaga, N.; Nguyen, K. A.; Su, S.; Windus, T. L.; Dupuis, M.; Montgomery, J. A. *J. Comput. Chem.* **1993**, *14*, 1347.

(40) Barbatti, M.; Ruckenbauer, M.; Lischka, H. *J. Chem. Phys.* **2005**, *122*, 174307.

(41) Hettema, H.; Yarkony, D. R. *J. Chem. Phys*, **1995**, *102*, 8431.

(42) Warshel, A. *Nature.* **1976**, *206*, 679.

(43) Matsika, S. *J. Phys. Chem. A* **2004**, *108*, 7584.

(44) Perun, S.; Sobolewski, A. L.; Domcke, W. *Mol. Phys.* **2006**, *104*, 1113.

(45) Ismail, N.; Blancafort, L.; Olivucci, M.; Kohler, B.; Robb, M. A. *J. Am. Chem. Soc.* **2002**, *124*, 6818.

(46) Sobolewski, A. L.; Woywod, C.; Domcke, W. *J. Chem. Phys.* **1993**, *98*, 5627.

(47) Perun, S.; Sobolewski, A. L.; Domcke, W. *J. Phys. Chem. A* **2006**, *110*, 13238.

(48) Kato, S. *J. Chem. Phys.* **1988**, *88*, 3045.

(49) Palmer, I. J.; Ragazos, I. N.; Bernardi, F.; Olivucci, M.; Robb, M. A. *J. Am. Chem. Soc.* **1993**, *115*, 673.

(50) Toniolo, A.; Thompson, A. L.; Martínez, T. J. *Chem. Phys.* **2004**, *304*, 133.

(51) Barbatti, M.; Vazdar, M.; Aquino, A. J. A.; Eckert-Maksić, M.; Lischka, H. *J. Chem. Phys.* **2006**, *125*, 164323.

(52) Michl, J.; Bonačić-Koutecký, V. *Electronic Aspects of Organic Photochemistry*; Wiley: New York, 1990.

(53) Barbatti, M.; Aquino, A. J. A.; Lischka, H. *Mol. Phys.* **2006**, *104*, 1053.

(54) (a) Barbatti, M.; Aquino, A. J. A.; Lischka, H. *J. Phys. Chem. A* **2005**, *109*, 5168. (b) Schreiber, M.; Barbatti, M.; Zilberg, S.; Lischka, H.; and González, L. *J. Phys. Chem. A* **2007**, *111*, 238.

(55) Zechmann, G.; Barbatti, M.; Lischka, H.; Pittner, J.; Bonačić-Koutecký, V. *Chem. Phys. Lett.* **2006**, *418*, 377.

(56) Bonačić-Koutecký, V.; Bruckmann, P.; Hiberty, P.; Koutecký, J.; Leforestier, C.; Salem, L. *Angew. Chem., Int. Ed. Engl.* **1975**, *14*, 575.

(57) Ohmine, I. *J. Chem. Phys.* **1985**, *83*, 2348.

(58) Barbatti, M.; Paier, J.; Lischka, H. *J. Chem. Phys.* **2004**, *121*, 11614.